

ENGINEERING DIVISION

Property of
Flood Control District of MC Library
LIBRARY DTIC FILE COPY
Please Return to
2801 MISCELLANEOUS PAPER HL-88-2

Phoenix, AZ 85009

NOMOGRAPHIC RIPRAP DESIGN

by

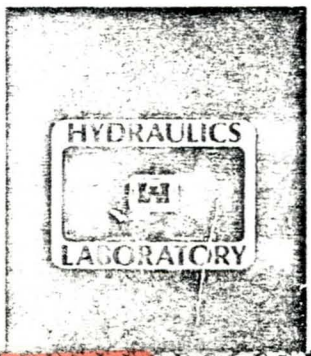
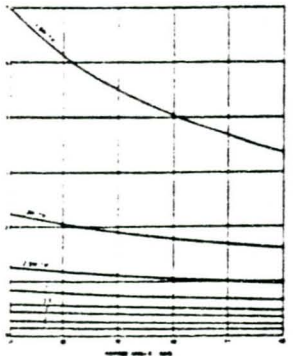
Andrew J. Reese

Hydraulics Laboratory

DEPARTMENT OF THE ARMY
Waterways Experiment Station, Corps of Engineers
PO Box 631, Vicksburg, Mississippi 39180-0631



AD-A195 328



March 1988
Final Report

Approved For Public Release; Distribution Unlimited

DTIC
ELECTE
MAY 03 1988
S H D

Prepared for DEPARTMENT OF THE ARMY
US Army Corps of Engineers
Washington, DC 20314-1000
Under Work Unit No. 31158

88 5 02 284

101.112

Library

LIBRARY

ENGINEERING DIVISION

DTIC FILE COPY

MISCELLANEOUS PAPER HL-88-2

NOMOGRAPHIC RIPRAP DESIGN

by

Andrew J. Reese

Hydraulics Laboratory

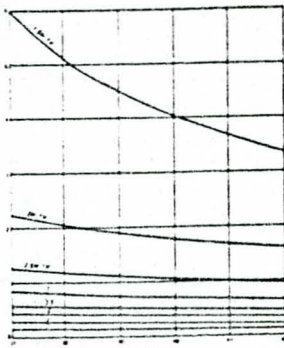
DEPARTMENT OF THE ARMY

Waterways Experiment Station, Corps of Engineers
PO Box 631, Vicksburg, Mississippi 39180-0631



US Army Corps
of Engineers

AD-A195 328



HYDRAULICS



LABORATORY



March 1988

Final Report

Approved For Public Release; Distribution Unlimited

DTIC
ELECTE
MAY 03 1988
S *at* H D

Prepared for DEPARTMENT OF THE ARMY
US Army Corps of Engineers
Washington, DC 20314-1000

Under Work Unit No. 31158

88 5_02 234

LIBRARY

ENGINEERING DIVISION

Destroy this report when no longer needed. Do not return
it to the originator.

The findings in this report are not to be construed as an official
Department of the Army position unless so designated
by other authorized documents.

The contents of this report are not to be used for
advertising, publication, or promotional purposes.
Citation of trade names does not constitute an
official endorsement or approval of the use of
such commercial products.

ENGINEERING DIVISION

Unclassified
SECURITY CLASSIFICATION OF THIS PAGE

REPORT DOCUMENTATION PAGE				Form Approved OMB No. 0704-0183	
1a. REPORT SECURITY CLASSIFICATION Unclassified			1b. RESTRICTIVE MARKINGS		
2a. SECURITY CLASSIFICATION AUTHORITY			3. DISTRIBUTION/AVAILABILITY OF REPORT Approved for public release; distribution unlimited.		
2b. DECLASSIFICATION/DOWNGRADING SCHEDULE			5. MONITORING ORGANIZATION REPORT NUMBER(S)		
4. PERFORMING ORGANIZATION REPORT NUMBER(S) Miscellaneous Paper HL-88-2			7a. NAME OF MONITORING ORGANIZATION		
6a. NAME OF PERFORMING ORGANIZATION USAEWES Hydraulic Laboratory		6b. OFFICE SYMBOL (if applicable) WESHP-D	7b. ADDRESS (City, State, and ZIP Code)		
6c. ADDRESS (City, State, and ZIP Code) PO Box 631 Vicksburg, MS 39180-0631			9. PROCUREMENT INSTRUMENT IDENTIFICATION NUMBER		
8a. NAME OF FUNDING/SPONSORING ORGANIZATION US Army Corps of Engineers		8b. OFFICE SYMBOL (if applicable)	10. SOURCE OF FUNDING NUMBERS See reverse		
8c. ADDRESS (City, State, and ZIP Code) Washington, DC 20314-1000			PROGRAM ELEMENT NO.	PROJECT NO.	TASK NO.
11. TITLE (Include Security Classification) Nomographic Riprap Design			WORK UNIT ACCESSION NO.		
12. PERSONAL AUTHOR(S) Reese, Andrew J.					
13a. TYPE OF REPORT Final report		13b. TIME COVERED FROM _____ TO _____		14. DATE OF REPORT (Year, Month, Day) March 1988	15. PAGE COUNT 50
16. SUPPLEMENTARY NOTATION Available from National Technical Information Service, 5285 Port Royal Road, Springfield, VA 22161.					
17. COSATI CODES			18. SUBJECT TERMS (Continue on reverse if necessary and identify by block number)		
FIELD	GROUP	SUB-GROUP	Nomographs Riprap design		
19. ABSTRACT (Continue on reverse if necessary and identify by block number)					
<p>→ This report presents a simplified design method for riprap sizing that allows adjustment of riprap size for specified safety factor, bend placement, side slope placement, specific weight, stone shape, channel shape effects, and roughness effects. It presents design nomographs for each of four sizing methods: Isbash, tractive force-logarithmic profile, tractive force-power profile, and Froude method. Method differences and advantages are explored. This report also discusses various practical riprap design considerations including transition design, strip roughness, and flow types. Examples are included.</p> <p style="text-align: center;">↑</p>					
20. DISTRIBUTION/AVAILABILITY OF ABSTRACT <input checked="" type="checkbox"/> UNCLASSIFIED/UNLIMITED <input type="checkbox"/> SAME AS RPT <input type="checkbox"/> DTIC USERS			21. ABSTRACT SECURITY CLASSIFICATION Unclassified		
22a. NAME OF RESPONSIBLE INDIVIDUAL			22b. TELEPHONE (include Area Code)		22c. OFFICE SYMBOL

DD Form 1473, JUN 85

Previous editions are obsolete.

SECURITY CLASSIFICATION OF THIS PAGE
Unclassified

A

Unclassified

SECURITY CLASSIFICATION OF THIS PAGE

10. WORK UNIT ACCESSION NO. (Continued).

Funding provided by the Flood Control Hydraulics Research Program, Work Unit No. 31158, Collection, Analysis, and Dissemination of Hydraulic Design Criteria Procedures, of the US Army Corps of Engineers.

Unclassified

SECURITY CLASSIFICATION OF THIS PAGE

PREFACE

The work described herein was performed by Mr. A. J. Reese, formerly of the Design Criteria Branch, Hydraulic Analysis Division, Hydraulics Laboratory, US Army Engineer Waterways Experiment Station (WES), with funding provided by the US Army Corps of Engineers through Work Unit No. 31158, Collection, Analysis, and Dissemination of Hydraulic Design Criteria Procedures, of the Flood Control Hydraulics Research Program.

This study was performed under the direction of Messrs. H. B. Simmons and F. A. Herrmann, Jr., former and present Chiefs of the Hydraulics Laboratory; Mr. M. B. Boyd, Chief of the Hydraulic Analysis Division; and Mr. B. J. Brown, Chief of the Design Criteria Branch. This report was edited by Mrs. Marsha C. Gay, Information Technology Laboratory.

Special acknowledgement is given to Messrs. J. L. Grace, Jr., former Chief, Hydraulic Structures Division; N. R. Oswalt, Chief, Spillways and Channels Branch; and S. T. Maynard, Spillways and Channels Branch, for their assistance and critical review during the preparation of this document.

COL Dwayne G. Lee, CE, is the Commander and Director of WES.
Dr. Robert W. Whalin is the Technical Director.



Accession For	
NTIS GRA&I	<input checked="" type="checkbox"/>
DTIC TAB	<input type="checkbox"/>
Unannounced	<input type="checkbox"/>
Justification	
By _____	
Distribution/	
Availability Codes	
Dist	Avail and/or Special
A-1	

CONTENTS

	<u>Page</u>
PREFACE.....	1
CONVERSION FACTORS, NON-SI TO SI (METRIC) UNITS OF MEASUREMENT.....	3
PART I: DEVELOPMENT.....	4
Introduction.....	4
Background.....	4
PART II: SOME RIPRAP DESIGN CONSIDERATIONS.....	10
Type I.....	10
Type II.....	10
Type III.....	11
Strip Sections.....	11
PART III: THE NOMOGRAPHIC METHOD.....	13
Basis of the Nomographic Method.....	13
Derivation.....	14
Power Profile.....	16
Froude and Isbash Methods.....	17
Logarithmic Profile... ..	17
Summary.....	18
Safety Factors.....	20
Shear Analysis.....	21
Computer Programs.....	22
REFERENCES.....	23
TABLE 1	
PLATES 1-13	
APPENDIX A: NOTATION.....	A1

CONVERSION FACTORS, NON-SI TO SI (METRIC)
UNITS OF MEASUREMENT

Non-SI units of measurement used in this report can be converted to SI
(metric) units as follows:

<u>Multiply</u>	<u>By</u>	<u>To Obtain</u>
cubic feet	0.02831685	cubic metres
degrees (angle)	0.01745329	radians
feet	0.3048	metres
inches	2.54	centimetres
pounds (mass) per cubic foot	16.01846	kilograms per cubic metre

NOMOGRAPHIC RIPRAP DESIGN

PART I: DEVELOPMENT

Introduction

1. This report presents a nomographic solution procedure for the design of riprap. The procedure incorporates five different riprap design methods and adjusts riprap size for (a) specified safety factor, (b) bend placement, (c) side slope placement, (d) a range of riprap specific weights, (e) stone shape, (f) use of hydraulic radius or local depth, and (g) specified roughness size. Examples are presented to illustrate the use of the nomographs.

Background

2. The development of the five methods of riprap design is presented in detail elsewhere (Reese 1984) and will only be summarized here.

Isbash method

3. By summing the forces on a stone, Isbash (1932, 1936) arrived at an equation which, presented in dimensionless form, is

$$\frac{\rho U_b^2}{(\gamma_s - \gamma) d_{50}} = 2K_I^2 \quad (1)$$

where

- ρ = mass density of water*
- U_b = velocity on the stone
- γ_s = specific weight of stone
- γ = specific weight of water
- d_{50} = median stone diameter
- K_I = empirical constant

* For convenience, symbols and abbreviations are listed in the Notation (Appendix A).

4. In areas where no velocity profile has been developed (e.g., below a structure), mean channel velocity V is commonly substituted for U_b . The value of K_I is generally taken as 0.86 for high turbulence locations and 1.2 for low turbulence locations (Office, Chief of Engineers (OCE), US Army, 1970).

Tractive force-logarithmic profile

5. The average boundary shear stress can be approximated by the following equation (OCE 1970)

$$\bar{\tau}_o = \frac{\gamma V^2}{\left(32.6 \log_{10} \frac{12.2pD'}{k_s}\right)^2} \quad (2)$$

where

$\bar{\tau}_o$ = average boundary shear, lb/ft²

p = multiple of depth such that hydraulic radius $R = pD'$

D' = depth to a fixed datum, ft

k_s = equivalent sand grain roughness of boundary, ft

6. This profile was originally derived using hydraulic radius R instead of depth D' (Keulegan 1938). Hydraulic radius, when used with mean channel velocity, accounts somewhat for the channel shape effects. Hydraulic radius is replaced by a multiple of depth (i.e., $R = pD'$, see Plate 11) in this and later equations. The value of p is taken equal to 1 when local mean depth is used with the corresponding mean velocity in the vertical \bar{v} to approximate shear at a point ($\bar{\tau}_o$). For all irregularly shaped cross sections it is recommended that local mean velocity above the stone be estimated and used instead of mean channel velocity. See Table 1 for further details.

7. Depth D' is measured from the free surface down to the assumed origin of the logarithmic profile. The original tractive force-logarithmic profile (OTFL) assumed depth to top of stone D for D' and d_{50} for k_s (OCE 1970). Evidence exists that the actual origin of the profile may be about d_{50} below the top of the rock layer and that k_s is somewhat greater than d_{50} . Using known riprap roughness measurements, k_s can be shown to be about $3d_{50}$ (although the value probably varies with depth, gradation, and shape) (Reese 1984, Hey 1979). D will be used for D' throughout the remainder of this report.

Modified tractive force-logarithmic profile

8. A modified profile (MTFL) can be developed for calculation purposes as

$$\bar{\tau}_o = \frac{\gamma V^2}{\left[32.6 \log_{10} \frac{12.2p}{m} \left(\frac{D}{d_{50}} + 1 \right) \right]^2} \quad (3)$$

where m is an empirical multiplier as

$$k_s = m d_{50} \quad (4)$$

Again, for local mean velocity $p = 1$ and local depth is used.

9. The critical tractive force is

$$\tau_c = K_T (\gamma_s - \gamma) d_{50} \quad (5)$$

where K_T is Shields's constant. The value of K_T may range from about 0.027 to 0.06 depending on flow conditions and definition of incipient motion.

10. At incipient motion $\bar{\tau}_o = \tau_c$. The OTFL (Equation 6) and MTFL (Equation 7) methods can then be derived as

$$\frac{\rho V^2}{(\gamma_s - \gamma) d_{50}} = K_T \left[5.75 \log_{10} \left(\frac{12.2pD}{m d_{50}} \right) \right]^2 \quad (6)$$

and

$$\frac{\rho V^2}{(\gamma_s - \gamma) d_{50}} = K_T \left\{ 5.75 \log_{10} \left[\frac{12.2p}{m} \left(\frac{D}{d_{50}} + 1 \right) \right] \right\}^2 \quad (7)$$

Tractive force-power profile

11. A power formula for $\bar{\tau}_o$ can be formed which closely approximates the logarithmic equation over the range $3 \leq R/k_s \leq 500$. It was shown (Reese 1984) that this equation actually fit available data better than the logarithmic profile and could be solved directly, whereas the logarithmic

equation requires an iterative procedure. The power form of $\bar{\tau}_o$ is

$$\bar{\tau}_o = \frac{\rho V^2}{63.39 \left(\frac{pD}{md_{50}} \right)^{1/3}} \quad (8)$$

12. Combined with Equation 5, the final dimensionless form is

$$\frac{\rho V^2}{(\gamma_s - \gamma) d_{50}} = 63.39 K_T \left(\frac{pD}{md_{50}} \right)^{1/3} \quad (9)$$

Froude number method

13. The Froude number method is commonly expressed as

$$\frac{d_{50}}{D} = K_F F^3 \quad (10)$$

where

K_F = empirical constant

F = flow Froude number (V/\sqrt{gD} where g = acceleration of gravity)

14. When this method is used, great reliance is placed on model studies and field experience for the determination of K_F . It is often used in areas of high or uncertain turbulence and in areas where flow configuration is controlled by a rapidly changing boundary (e.g., below structures). K_F ranges from 0.22 for incipient motion in flume studies, to 0.35 for channel design, to as high as 7.5 for low-head navigation structures where energy dissipation is poor (Maynard 1978; Grace, Calhoun, and Brown 1973). A value of 1.0 is recommended for structures with effective energy dissipation.

15. Equation 9 can be rearranged as

$$\left[\frac{\gamma_m^{1/3}}{(\gamma_s - \gamma) 63.39 K_T^{1/3}} \right]^{3/2} \left[\frac{V}{(gD)^{1/2}} \right]^3 = \frac{d_{50}}{D} \quad (11)$$

This is the same form as Equation 10. K_F is equivalent to the left-hand term. Thus the Froude method can be thought of as a simplified tractive

force-power (TFP) profile. What is gained in simplicity of expression is lost in flexibility of input.

16. K_F is then

$$K_F = \left[\frac{\gamma_m^{1/3}}{(\gamma_s - \gamma) 63.39 K_T P^{1/3}} \right]^{3/2} \quad (12)$$

Solving for K_T with $\gamma_s = 165 \text{ lb/cu ft}^*$ and $\gamma = 62.4 \text{ lb/cu ft}$ gives

$$K_T = \frac{1}{104.23 K_F^{2/3}} \left(\frac{m}{p} \right)^{1/3} \quad (13)$$

Substitution into Equation 9 gives the appropriate dimensionless form:

$$\frac{\rho V^2}{(\gamma_s - \gamma) d_{50}} = \frac{1}{1.65 K_F^{2/3}} \left(\frac{D}{d_{50}} \right)^{1/3} \quad (14)$$

K_F intrinsically incorporates the p and m adjustments.

Method summary

17. The five equations for riprap design are then (using $V = U_b$):

Irbash:
$$\frac{\rho V^2}{(\gamma_s - \gamma) d_{50}} = 2 K_I^2 \quad (1)$$

OTFL:
$$\frac{\rho V^2}{(\gamma_s - \gamma) d_{50}} = K_T \left[5.75 \log_{10} \left(\frac{12.2 p D}{m d_{50}} \right) \right]^2 \quad (6)$$

MTFL:
$$\frac{\rho V^2}{(\gamma_s - \gamma) d_{50}} = K_T \left\{ 5.75 \log_{10} \left[\frac{12.2 p}{m} \left(\frac{v}{d_{50}} + 1 \right) \right] \right\}^2 \quad (7)$$

* A table of factors for converting non-SI units of measurement to SI (metric) units is found on page 3.

TFP:
$$\frac{\rho v^2}{(\gamma_s - \gamma) d_{50}} = 63.39 K_T \left(\frac{\rho D}{m d_{50}} \right)^{1/3} \quad (9)$$

Froude:
$$\frac{\rho v^2}{(\gamma_s - \gamma) d_{50}} = \frac{1}{1.65 K_F^{2/3}} \left(\frac{D}{d_{50}} \right)^{1/3} \quad (14)$$

PART II: SOME RIPRAP DESIGN CONSIDERATIONS

18. In the design of riprap stone size, any of three flow situations or types may predominate. Depending on the situation, a slightly different design method is used. The three types are (a) upstream roughness dependence (Type I), (b) riprap roughness dependence (Type II), and (c) boundary geometry dependence (Type III).

Type I

19. In a Type I situation, flow moves from an upstream channel reach of lesser roughness into the riprap-protected reach. An example might be transition from a concrete-lined section to a riprap-protected section. If the upstream roughness is greater than that of the riprap, Type II methods should be used. It can be shown that if the riprap protrudes above the upstream bed by more than a small amount or if the roughness difference is great, there will be a transition section in which the forces attempting to dislodge the stone will be greater than further downstream where the velocity at the top of the level of the rock has been slowed. In Type I flow, the velocity of the upstream reach should be used to size the stone in this transition section. In many cases the velocity entering the section is sufficiently close to the eventual velocity within the section that Types I and II riprap design methods will yield approximately equal d_{50} sizes. If the length of the transition section is assumed equal to the distance required to submerge the stone in a turbulent boundary layer initiated at the upstream edge of the riprap section, the transition section length can be estimated to be 75 to 100 times d_{50} .

Type II

20. Type II flow is used if upstream and protected section roughness are somewhat similar and riprap does not greatly protrude into the flow (thus creating a smooth transition), or for protected sections downstream from a transitional section when the velocity in the channel and the size of stone are interdependent. In this case an iterative solution is required. A size is first chosen and velocity calculated. Then this velocity is used to determine a stable riprap size. The initial and calculated sizes are compared and

the procedure repeated until approximate agreement is reached.

Type III

21. In Type III flow, the velocity distribution is largely determined by the boundary geometry. Turbulence caused by, for example, expansions, contractions, drops, or sills predominates. In these cases the refinements of velocity profile are overshadowed by boundary-generated macroturbulence. A judicious choice of empirical constant is then the most important factor in stone sizing. The Froude or Isbash methods are usually used in Type III situations because of their simplicity. Often model studies are recommended if the flow conditions are unique and the importance of the structure warrants the added cost.

Strip Sections

22. Often the channel perimeter is not uniformly protected. The banks may be protected and the bed left in its natural or excavated state. If a large side slope is to be protected, the riprap size may be decreased in longitudinal strips up the bank as a cost-saving measure.

23. Although the actual scour mechanism is not well understood in these cases, the toe of the bank or the lower portion of the riprap strip is usually most vulnerable to scour or stone displacement. Some methods for toe protection are discussed in Engineer Manual 1110-2-1601 (OCE 1970). Actual required toe depth is quite variable and depends on stream type, flow angle, bed and bank material, and history. It is sometimes calculated to be the sum of general and local scour plus one-half the anticipated bed form height.

24. The normal method of approach (short of two-dimensional mathematical modeling but beyond simply using mean channel velocity) when roughness varies in longitudinal strips is first to calculate the mean velocity in each strip (e.g., using a suitable backwater program for gradually varied flow or the alpha method (OCE 1970) for uniform flow). It is then assumed that the faster velocity of an adjacent strip impinges on a section of slower velocity at unknown and varying points. For example, the faster velocity in the center portion of a channel with protected banks is used to size the riprap on the bank, or the faster velocity on a lower portion of a bank is used to size the

riprap on an adjacent upper portion of the bank. These methods are illustrated in Table 1.

25. The built-in safety factor incurred by using this method will, for steeper slopes and shallower flows, give unrealistically large riprap sizes. For certain combinations of variables no solution can be found for the logarithmic methods. It is probably best, in these situations, to reconsider whether riprap is an appropriate form of bed or bank protection and, if it is, to choose a size based on experience or velocity measurement.

PART III: THE NOMOGRAPHIC METHOD

Basis of the Nomographic Method

26. The Nomographic Method is an attempt to provide a simple-to-use yet accurate method for riprap sizing. It has an additional advantage in that it also provides a design engineer with a visual "feel" for the relative sensitivity of various assumptions and placement situations used in design.

27. The basic concept of this method is illustrated by Plate 1. For a given set of conditions, a velocity versus depth plot can be drawn using a family of d_{50} curves. The designer simply finds the intersection of known velocity and depth and reads the appropriate d_{50} size directly. Plate 1 uses the OTFL equation (Equation 6) for a stated set of "base conditions." The problem is that there is an infinite number of combinations of conditions each of which would generate a different family of curves. For example, if the riprap is placed on a side slope, the family of curves would shift to the left, requiring a larger d_{50} size for the same velocity and depth.

28. Rather than shifting the d_{50} curves to the left (or right) when departures from base conditions are encountered, in the nomographic method, the velocity is shifted. The question can be asked, "What velocity would result in the same d_{50} size using the base condition family of curves (Plate 1 here) as would be obtained by plotting a new family of curves for the new set of conditions?"

29. A departure from any of the base conditions (Plates 1-5) is accounted for by an adjustment to the real-world velocity, creating a fictitious velocity. That is, any factor which increases or decreases the ability of a stone to remain stationary can be reflected by a corresponding decrease or increase in velocity. This fictitious new velocity is called the "effective velocity." Thus, through coefficients obtained from Plates 6-13, the user moves either to the right or left of the actual velocity on the velocity scale and then moves upward to the calculated depth and reads the d_{50} size.

30. The base conditions (Plates 1-5) can be adjusted for riprap shape, side slope or bend placement, specific weight changes, use of different constant values or safety factors, use of hydraulic radius (channel shape), and use of different equivalent sand grain roughnesses. Examples in Table 1 illustrate adjustments to the base conditions. The following base conditions

are used in Plates 1-5: moderately angular riprap placed on the bed of a straight channel, $\gamma_s = 165 \text{ lb/cu ft}$, $k_s = d_{50}$, D is used instead of R , and base values for the constants are used ($K_T = 0.04$, $K_F = 0.22$, $K_I = 1.2$).

31. The tractive stress displacement methods depend on an accurate description of the vertical velocity profile to be able to transpose a known velocity to a bed shear stress. When the bed roughness elements are large in relation to the flow depth (between 1/10 to 1/3), the methods begin to lose accuracy due to roughness shape and free surface effects. These effects tend to increase the friction factor (slow the velocity) and thus lead to a more conservative design. The dashed lines on Plates 1-5 indicate a D/d_{50} value of 3 (roughness elements = 1/3 depth). These charts should not be used for design below this value as variation from profile assumptions reaches unacceptable levels.

Derivation

32. At incipient motion $\bar{\tau}_o = \tau_c$. Several factors may increase actual shear ($\bar{\tau}_o$) or decrease critical shear (τ_c).

Bend placement

33. The maximum shear in a bend (OCE 1970) can be expressed as

$$\tau_b = \bar{\tau}_o \left[3.12 \left(\frac{T}{R_c} \right)^{0.5} \right] \quad (15)$$

where

τ_b = shear in a bend

T = top width of channel entering bend

R_c = centerline radius of curvature of bend

or

$$\tau_b = \bar{\tau}_o K_B \quad (16)$$

where K_B , the coefficient for bend shear, is the term in brackets in Equation 15.

Side slope placement

34. The required critical shear for side slope placement (OCE 1970) is expressed as

$$\tau_s = \tau_c \left[\left(1 - \frac{\sin^2 \phi}{\sin^2 \theta} \right)^{1/2} \right] \quad (17)$$

or

$$\tau_s = \tau_c K_s \quad (18)$$

where

τ_s = side slope critical shear

ϕ = side slope angle

θ = riprap angle of repose

K_s = coefficient of side slope shear (bracketed term in Equation 17)

Safety factor

35. The safety factor is expressed as

$$\tau_{SF} = \bar{\tau}_o K_{SF} \quad (19)$$

where

τ_{SF} = actual shear with a safety factor applied

K_{SF} = safety factor

A factor of 1.5 had been recommended for moderate nonuniformity in plan, profile, or roughness (OCE 1971).

36. All of these factors can be applied independently (although the bend correction equation incorporates about a 1.5 safety factor with it when compared with straight channel design) at the discretion of the designer.

Thus

$$\bar{\tau}_o K_B K_{SF} = \tau_c K_s \quad (20)$$

or

$$\bar{\tau}_o = \frac{K_s}{K_B K_{SF}} \tau_c \quad (21)$$

Power Profile

37. Remembering that $k_s = md_{50}$ and $R = pD$ and using γ'_s to represent a specific weight of stone other than 165 lb/cu ft (base condition), Equations 5 and 8 are substituted into 21 for $\bar{\tau}_o$ and τ_c , respectively, and rearranged to give

$$V = \left[\frac{63.39 K'_T (\gamma'_s - \gamma) d_{50} K_s}{K_B \rho} \right]^{1/2} \left(\frac{pD}{md_{50}} \right)^{1/6} \quad (22)$$

where K'_T is the use of a constant other than the base constant. K'_T combines K_T and K_{SF} such that $K'_T = K_T / K_{SF}$. Thus a choice of K'_T of 0.027 is equivalent to a shear safety factor of 1.5 ($0.027 = 0.04/1.5$) and so on.

38. The variable V in Equation 22 is the actual velocity. The effective velocity is that which will give the same d_{50} for the same depth but for base conditions. It is expressed as

$$V_{eff} = \left[\frac{63.39 K_T (\gamma_s - \gamma) d_{50}}{\rho} \right]^{1/2} \left(\frac{D}{d_{50}} \right)^{1/6} \quad (23)$$

where the base value for K_T is 0.04 and γ_s is 165 lb/cu ft.

39. Dividing Equation 23 by 22 gives

$$\frac{V_{eff}}{V} = \left(\frac{0.04}{K'_T} \right)^{1/2} \left[\frac{102.6}{(\gamma'_s - \gamma)} \right]^{1/2} \left(\frac{K_B}{K_s} \right)^{1/2} \left(\frac{m}{p} \right)^{1/6} \quad (24)$$

or

$$V_{eff} = C_t C_g C_b C_s C_m C_p V \quad (25)$$

where

$$C_t = \left(\frac{0.04}{K_T} \right)^{1/2}$$

$$C_g = \left[\frac{102.6}{(\gamma_s - \gamma)} \right]^{1/2}$$

$$C_b = K_B^{1/2}$$

$$C_s = \left(\frac{1}{K_s} \right)^{1/2}$$

$$C_m = m^{1/6}$$

$$C_p = \left(\frac{1}{p} \right)^{1/6}$$

Thus for any given set of conditions the user determines the correction coefficients and multiplies them times the given velocity to obtain an effective velocity. He then reads the d_{50} size directly from the intersection point of effective velocity and depth.

Froude and Isbash Methods

40. Because of the nature of the Froude and Isbash methods, the C_p and C_m corrections are not applicable to them. Side slope and bend corrections are not applicable to the Isbash method in its original derivation.

Logarithmic Profile

41. The logarithmic profile can be arranged similar to the power profile giving

$$v = 5.75 \left[\frac{K_s K_T' (\gamma_s' - \gamma) d_{50}}{K_B \rho} \right]^{1/2} \left[\log_{10} \left(\frac{12.2 p D}{m d_{50}} \right) \right] \quad (26)$$

and

$$v_{\text{eff}} = 5.75 \left[\frac{K_T (\gamma_s - \gamma) d_{50}}{\rho} \right]^{1/2} \left[\log_{10} \left(\frac{12.2 D}{d_{50}} \right) \right] \quad (27)$$

Dividing Equation 27 by Equation 26 gives

$$\frac{v_{\text{eff}}}{v} = \left(\frac{0.04}{K_T'} \right)^{1/2} \left[\frac{(102.6)}{\gamma_s' - \gamma} \right]^{1/2} \left(\frac{K_B}{K_s} \right)^{1/2} \left[\frac{\log_{10} \left(\frac{12.2 D}{d_{50}} \right)}{\log_{10} \left(\frac{12.2 p D}{m d_{50}} \right)} \right] \quad (28)$$

or

$$v_{\text{eff}} = C_t C_g C_b C_s C v \quad (29)$$

where C_t , C_g , C_b , and C_s are as defined following Equation 25 and

$$C = \frac{\log_{10} \left(\frac{12.2 D}{d_{50}} \right)}{\log_{10} \left(\frac{12.2 p D}{m d_{50}} \right)} \quad (30)$$

C carries with it the correction for both hydraulic radius and equivalent roughness and was arranged in this way to provide multiplicative rather than additive corrections. For local velocity use set $R = D$ (the extreme top of the chart).

Summary

42. The various coefficients used to adjust the actual velocity can now

be summarized. These equations may be used in lieu of the plates if greater accuracy is desired.

- a. Stone shape and side slope placement C_s corrections are found in Plates 6 and 7, respectively, and expressed as

$$C_s = \left(1 - \frac{\sin^2 \phi}{\sin^2 \theta} \right)^{-1/4} \quad (31)$$

Plate 6 was developed from work by Simons (1957) and is used to estimate angle of repose.

- b. The bend correction, found in Plate 8, is expressed as

$$C_b = 1.77 \left(\frac{T}{R_c} \right)^{1/4} \quad (32)$$

- c. The specific weight correction is found from Plate 9 and expressed as

$$C_g = \left[\frac{102.6}{(\gamma_s' - 62.4)} \right]^{1/2} \quad (33)$$

- d. The constant correction coefficient for each of the four methods is found in Plate 10. For the power and logarithmic profiles it is given as

$$C_t = \left(\frac{0.04}{K_T'} \right)^{1/2} \quad (34)$$

For the Isbash method it is

$$C_i = \frac{1.2}{K_I'} \quad (35)$$

where K_I' is the chosen Isbash constant. For the Froude method it is

$$C_f = \left(\frac{K_F'}{0.22} \right)^{1/3} \quad (36)$$

where K'_F is the chosen Froude constant.

- e. The channel shape correction factor for the power profile is found in Plate 11 for a known top width, depth, and side slope. It is given as

$$C_p = \left(\frac{1}{P}\right)^{1/6} \quad (37)$$

- f. The correction for both shape of channel and equivalent roughness for the logarithmic profiles is given in Plate 12 and as

$$C = \frac{\log_{10} \left(\frac{12.2D}{d_{50}} \right)}{\log_{10} \left(\frac{12.2pD}{md_{50}} \right)} \quad (38)$$

The depth used here depends on which logarithmic method will be used. The OTFL method uses depth to top of rock while the MTL method uses depth to d_{50} below top of rock. Therefore use $D/d_{50} + 1$ in place of D/d_{50} in both numerator and denominator of Equation 38 for the MTL method.

- g. Plate 13 gives the power profile correction for equivalent roughness as

$$C_m = m^{1/6} \quad (39)$$

Safety Factors

43. Safety factors (OCE 1971) for the logarithmic and power profiles are found from

$$SF_T = \frac{0.04}{K'_T} \quad (40)$$

where SF_T is the shear safety factor. For the Froude method, assuming 0.22 to be the ideal situation incipient motion constant, it is found that

$$SF_F = \left(\frac{K'_F}{0.22} \right)^{2/3} \quad (41)$$

These are shear safety factors. For example: to provide the recommended 1.5 safety factor on the calculated actual shear, K'_T must be 0.027 and K'_F must be 0.404.

Shear Analysis

44. Insight can be gained by returning to the original premise for shear-induced riprap instability of paragraph 10. At incipient motion the shear acting on a stone equals the critical shear for movement or $\bar{\tau}_o = \tau_c$. Equation 20 demonstrated in a preliminary way the relationship between the actual and critical shears $\bar{\tau}_o$ and τ_c , and the various factors affecting them. By combining Equations 31-38 (the factors read directly from the nomograph) with the definitions for the shears, a nomographic shear analysis can be performed, identical to the method given in EM 1110-2-1601 (OCE 1970).

45. For the OTFL method the proper equation is

$$\frac{\gamma V^2}{\left(32.6 \log_{10} \frac{12.2D}{d_{50}} \right)^2} (C_b C_t C)^2 = 4.10 d_{50} \left(\frac{1}{C_s C_g} \right)^2 \quad (42)$$

Here, and in the two equations following, the form of the equation is

$$\bar{\tau}_{o\text{eff}} = \tau_{c\text{eff}} \quad (43)$$

The left side is the actual shear adjusted for channel shape, bend, equivalent roughness, and safety factor. The right side of the equation is the critical shear adjusted for specific weight and side slope placement.

46. The equation for the MTFM method is

$$\frac{\gamma V^2}{\left\{ 32.6 \log_{10} \left[12.2 \left(\frac{D}{d_{50}} + 1 \right) \right] \right\}^2} (C_b C_t C)^2 = 4.10 d_{50} \left(\frac{1}{C_s C_g} \right)^2 \quad (44)$$

47. The equation for the power profile method is

$$\frac{\gamma V^2}{63.69g \left(\frac{D}{d_{50}}\right)^{1/3}} (C_b C_t C_p C_m)^2 = 4.10 d_{50} \left(\frac{1}{C_s C_g}\right)^2 \quad (45)$$

Computer Programs

48. A computer program which allows for on-line, interactive riprap design using the methods presented in this paper is available at all US Army Corps of Engineers design offices through the Conversationally-Oriented Real-Time Programming System (CORPS). It is entitled H7011-Riprap Design by Four Methods. For complete documentation and information, contact the Engineer Computer Programs Library (WESIM-SC) at FTS 542-2581.

REFERENCES

- Grace, J. L., Calhoun, C. C., and Brown, D. N. 1973 (Jun). "Drainage and Erosion Control Facilities, Field Performance Investigation," Miscellaneous Paper H-73-6, US Army Engineer Waterways Experiment Station, Vicksburg, Miss.
- Hey, R. D. 1979 (Apr). "Flow Resistance in Gravel Bed Rivers," Journal of the Hydraulics Division, American Society of Civil Engineers, Vol 105, No. HY4, pp 365-379.
- Isbash, S. V. 1932. Construction of Dams by Dumping Stones in Flowing Water, Leningrad, Translated by A. Dorijikov, US Army Engineer District, Eastport, Maine, 1935.
- _____. 1936. "Construction of Dams by Depositing Rocks in Running Water," Transactions, Second Congress on Large Dams, Vol 5, pp 123-136.
- Keulegan, G. H. 1938 (Dec). "Laws of Turbulent Flow in Open Channels," Research Paper 1151, US National Bureau of Standards, Vol 21.
- Maynard, S. T. 1978 (Jun). "Practical Riprap Design," Miscellaneous Paper H-78-7, US Army Engineer Waterways Experiment Station, Vicksburg, Miss.
- Office, Chief of Engineers, US Army. 1970 (1 Jul). "Hydraulic Design of Flood Control Channels," EM 1110-2-1601, US Government Printing Office, Washington, DC.
- _____. 1971 (14 May). "Additional Guidance for Riprap Protection," ETL 1110-2-120, US Government Printing Office, Washington, DC.
- Reese, A. J. 1984. "Riprap Sizing - Four Methods," Proceedings of Hydraulics Specialty Conference, American Society of Civil Engineers, Coeur d'Alene, Idaho, pp 397-401.
- Simons, D. B. 1957. "Theory and Design of Stable Channels in Alluvial Material," Ph.D. dissertation, Colorado State University, Department of Civil Engineering, Fort Collins, Colo.

Table 1

Examples

Example 1: Type I Flow--Bend Placement

Given: $R_c = 200$ ft $D = 8$ ft $k_s = 2d_{50}$
 $T = 50$ ft $V = 11$ fps $\gamma_s = 175$ lb/cu ft

Side Slope = 2H:1V

Moderately rounded stone, trapezoidal channel

Use TFP method and mean channel velocity (upstream)

Step 1. Side Slope Correction

Assume $d_{50} = 15$ in. $\phi = 26.6$ deg $K'_T = 0.027$ (1.5 safety factor)

From Plate 6: $\theta = 40.5$ deg

From Plate 7: $C_s = 1.17$

Step 2. Bend Correction

$T/R_c = 50/200 = 0.25$

From Plate 8: $C_b = 1.25$

Step 3. Specific Weight Correction

From Plate 9: $C_g = 0.95$

Step 4. Power Profile Channel Shape Correction

$T/D = 50/8 = 6.25$

From Plate 11: $C_p = 1.07$

Step 5. Equivalent Sand Grain Roughness Correction, Power Profile

$m = 2$

From Plate 13: $C_m = 1.12$

Step 6. Safety Factor

$K'_T = 0.027$

(Continued)

(Sheet 1 of 5)

Table 1 (Continued)

From Plate 10: $C_t = 1.22$

Step 7. Power Profile

$$V_{\text{eff}} = C_s C_b C_g C_p C_m C_t V$$

$$= (1.17)(1.25)(0.95)(1.07)(1.12)(1.22)(11)$$

$$= 22.34 \text{ fps}$$

From Plate 4: $d_{50} = 31 \text{ in.}$

Step 8. Check Side Slope Correction

$$d_{50} = 31 \text{ in.} \quad \phi = 26.6 \text{ deg} \quad K'_T = 0.027$$

From Plate 6: $\theta = 41.0 \text{ deg}$

From Plate 7: $C_s = 1.17$

The side slope correction does not change so the rock size $d_{50} = 31 \text{ in.}$ is correct.

Example 2: Type I Flow--Transition Design

Given: $Q = 4,000 \text{ cfs}$ Bottom width = 50 ft $\gamma_s = 165 \text{ lb/cu ft}$

Bottom Slope = 0.00082 2H:1V Side Slopes

A. Concrete Section

Manning's $n = 0.012$ V (mean) = 10.75 fps

$D = 6 \text{ ft}$ V (center) = 11.69 fps

V (sides) = 6.84 fps

B. Transition Section

Assume a fairly smooth transition

Power method $k_s = 3d_{50}$ $K'_T = 0.027$ (1.5 safety factor)

Step 1. Side Slope Correction

Assuming $d_{50} = 24 \text{ in.}$

(Continued)

Table 1 (Continued)

- From Plate 6: $\theta = 41.5$ deg (moderately angular stone)
- From Plate 7: $C_s = 1.16$
- Step 2. Safety Factor
- From Plate 10: $C_t = 1.22$
- Step 3. $k_s = 3d_{50}$
- From Plate 13: $C_m = 1.20$
- Step 4. $V_{eff} = V(C_s)(C_t)(C_m) = (11.69)(1.16)(1.22)(1.20) = 19.85$ fps
- From Plate 4: $d_{50} = 25$ in.
- Step 5. Assume approximate transition zone distance of $75d_{50} = 150$ ft .

C. Downstream Section Size Check

Assume $n = 0.030$ (conservative)

Then V (center) = 6.54 fps V (mean) = 5.77 fps

$D = 9.93$ ft

$d_{50} = 3.5$ in.

D. The designer now has the choice of how to step down the size from 24 in. to an unprotected section. The 24-in. size will be carried 100 ft downstream with a 12-in. stepdown for an additional 50 ft with tie-ins.

Example 3: Type II Flow--Side Slope Placement

Given: $Q = 8,000$ cfs Bottom width = 70 ft

2H:1V side slopes Bottom slope = 0.0040

Bottom roughness: Manning's $n = 0.028$

$\gamma_s = 165$ lb/cu ft (moderately angular stone)

Assume uniform flow $k_s = 2d_{50}$

1.5 safety factor

(Continued)

(Sheet 3 of 5)

Table 1 (Continued)

Size stone for bank protection using power profile method and sectional velocities.

- Step 1. Determine applicable velocities and depth. Using CORPS program H7012 - The Alpha Method:

Assuming Manning's $n = 0.04d_{50}^{1/6}$ (d_{50} in feet) and $d_{50} = 12$ in.

Manning's $n = 0.04$ on protected slopes

Center velocity = 13.28 fps

Depth = 7.88 ft

Side slope velocity = 5.44 fps

- Step 2. Side slope correction

From Plate 6: Repose angle = 41 deg

From Plate 7: $C_s = 1.17$

- Step 3. Equivalent roughness correction

From Plate 13 ($m = 2$): $C_m = 1.12$

- Step 4. Safety factor correction

From Equation 40 for $SF_T = 1.5$: $K_T' = 0.027$

From Plate 10: $C_t = 1.22$

- Step 5. $V_{eff} = (1.17)(1.12)(1.22)(13.28) = 21.32$ fps

From Plate 4: $d_{50} = 26$ in.

- Step 6. Recalculate downstream velocity using larger d_{50} size

Manning's $n = 0.04(26/12)^{1/6} = 0.045$

Using H7012

Velocity center = 13.33 fps

Velocity bank = 4.85 fps

Depth = 7.92 ft

(Continued)

Table 1 (Concluded)

Step 7. Recalculate d_{50} size

$$V_{\text{eff}} = (1.17)(1.12)(1.22)(13.33) = 21.31 \text{ fps}$$

From Plate 4: $d_{50} = 27 \text{ in. (OK)}$

Example 4: Type III Flow--Basin Design

Flow below drop structure. Use Isbash and Froude methods.

V (over end sill) = 12.4 fps

$D = 11 \text{ ft}$

$\gamma = 185 \text{ lb/cu ft}$

3H:1V side slopes with moderately angular stone

K'_I and K'_F are selected based on experience

Step 1. Specific weight correction

From Plate 9: $C_g = 0.91$

Step 2. Side slope correction (Froude only)

From Plate 6: $\theta = 41.5 \text{ deg}$

From Plate 7: $C_s = 1.07$

Step 3. From Plate 10: $C_i = 1.39$ for $K'_I = 0.86$ (for high-turbulence location)

$C_f = 1.65$ for $K'_F = 1.00$ (for structures with effective energy dissipation)

Step 4. Isbash

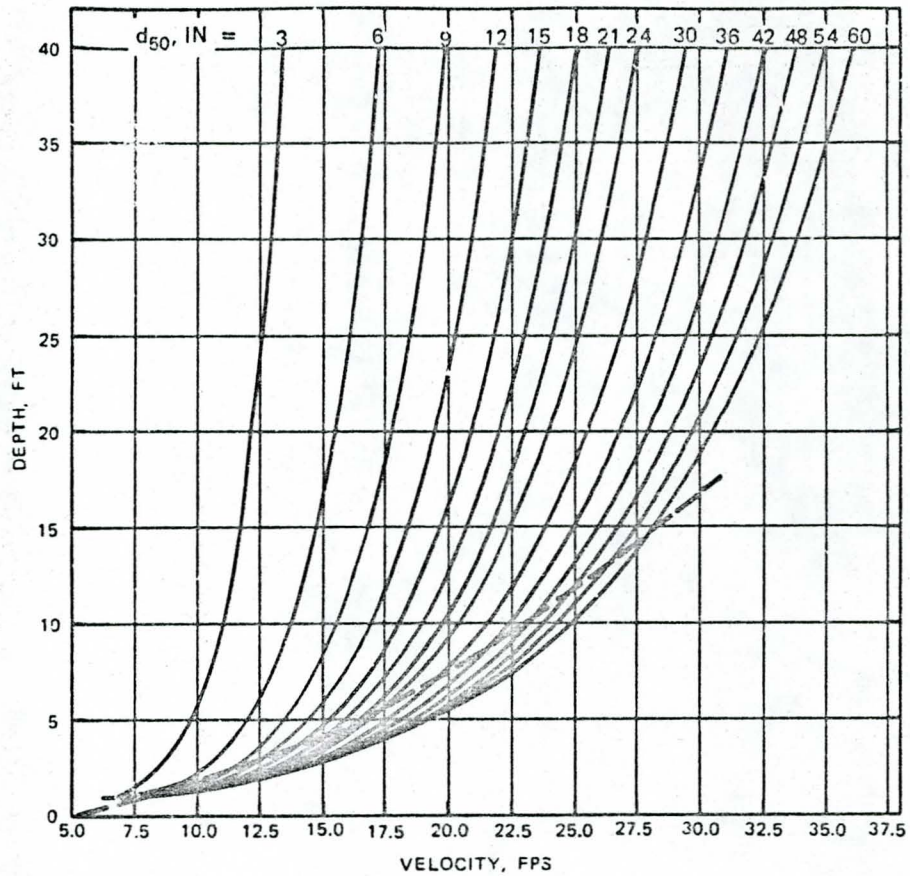
$$V_{\text{eff}} = VC_g C_i = (12.4)(0.91)(1.39) = 15.68 \text{ fps}$$

$d_{50} = 20 \text{ in.}$

Froude

$$V_{\text{eff}} = VC_g C_f C_s = (12.4)(0.91)(1.65)(1.07) = 19.92 \text{ fps}$$

$d_{50} = 36 \text{ in.}$



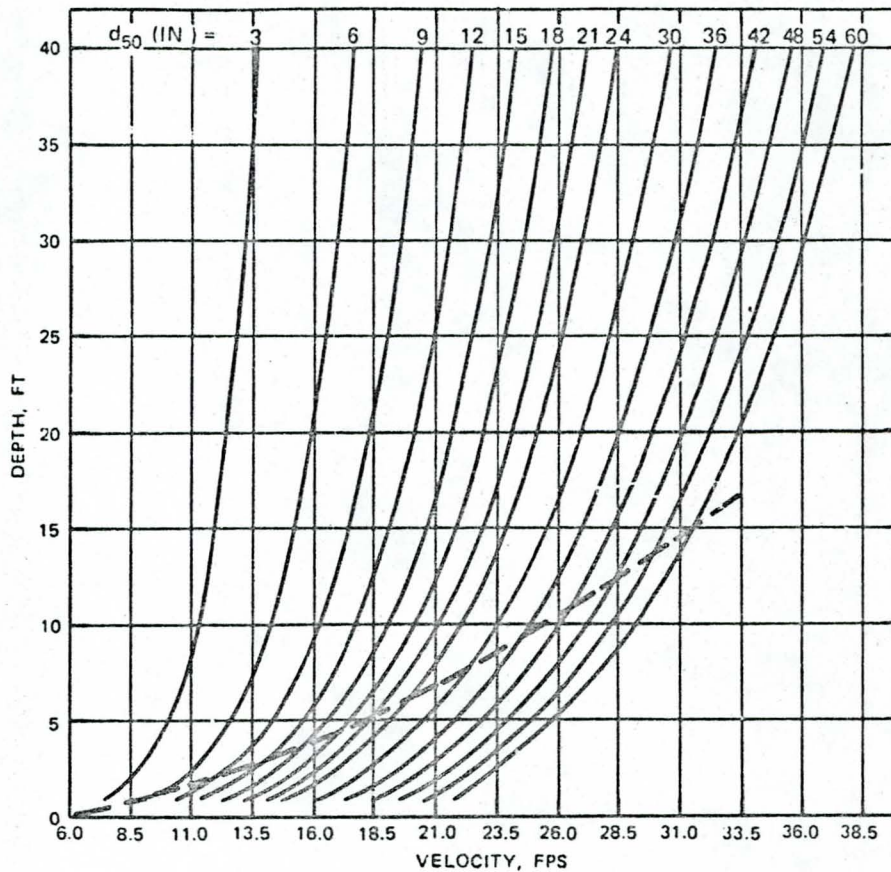
$$\frac{\rho V^2}{(\gamma_s - \gamma)d_{50}} = K_t \left[5.75 \text{ LOG} \left(\frac{12.2D}{k_s} \right) \right]^2$$

BASE VALUES

$\gamma_s = 165 \text{ LB/CU FT}$
 $K_T = 0.04$
 $k_s = d_{50}$
 LOCAL DEPTH
 MODERATELY ANGULAR STONE
 STRAIGHT CHANNEL
 BED PLACEMENT

NOTE: METHOD LOSES ACCURACY BELOW DASHED LINE DUE TO FREE SURFACE EFFECTS

STONE STABILITY
TRACTIVE FORCE-LOGARITHMIC PROFILE
CRITICAL MEAN VELOCITY
VS. MEAN DEPTH



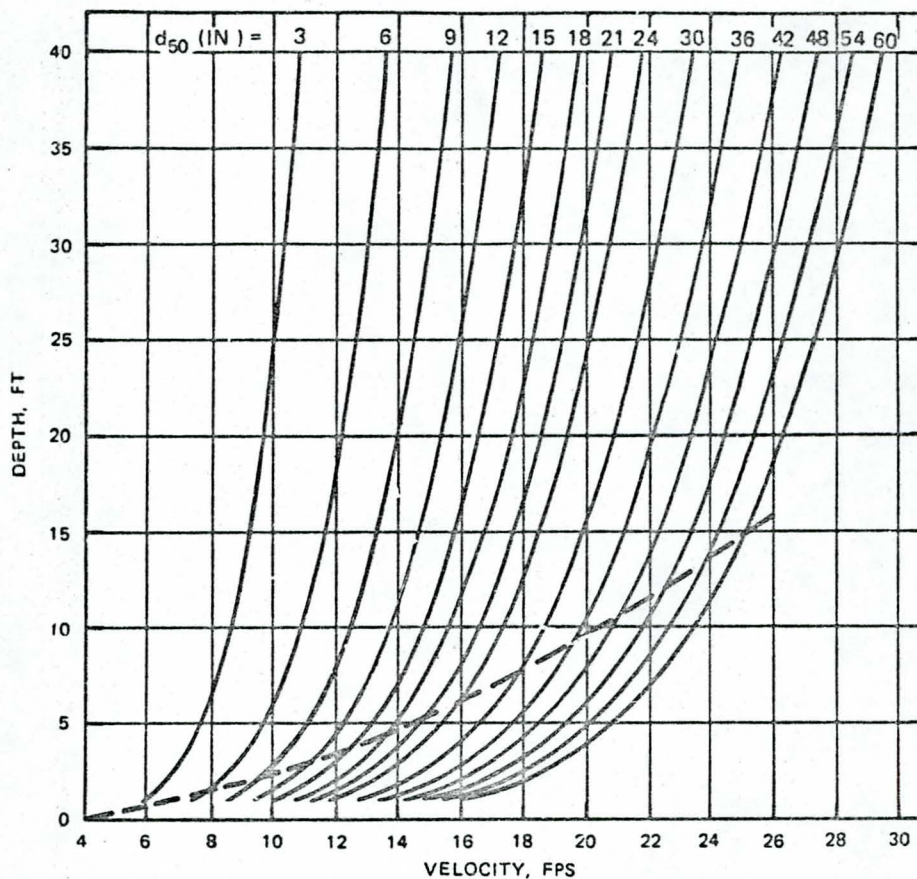
$$\frac{\rho V^2}{(\gamma_s - \gamma) d_{50}} = K_t \left\{ 5.75 \text{ LOG} \left[\frac{12.2}{k_s} (D + d_{50}) \right] \right\}^2$$

BASE VALUES

$\gamma_s = 165 \text{ LB/CU FT}$
 $K_T = 0.04$
 $k_s = d_{50}$
 LOCAL DEPTH
 MODERATELY ANGULAR STONE
 STRAIGHT CHANNEL
 BED PLACEMENT

NOTE: METHOD LOSES ACCURACY BELOW
 DASHED LINE DUE TO FREE SURFACE
 EFFECTS

STONE STABILITY
TRACTIVE FORCE-LOGARITHMIC PROFILE
MODIFIED
CRITICAL MEAN VELOCITY
VS. MEAN DEPTH



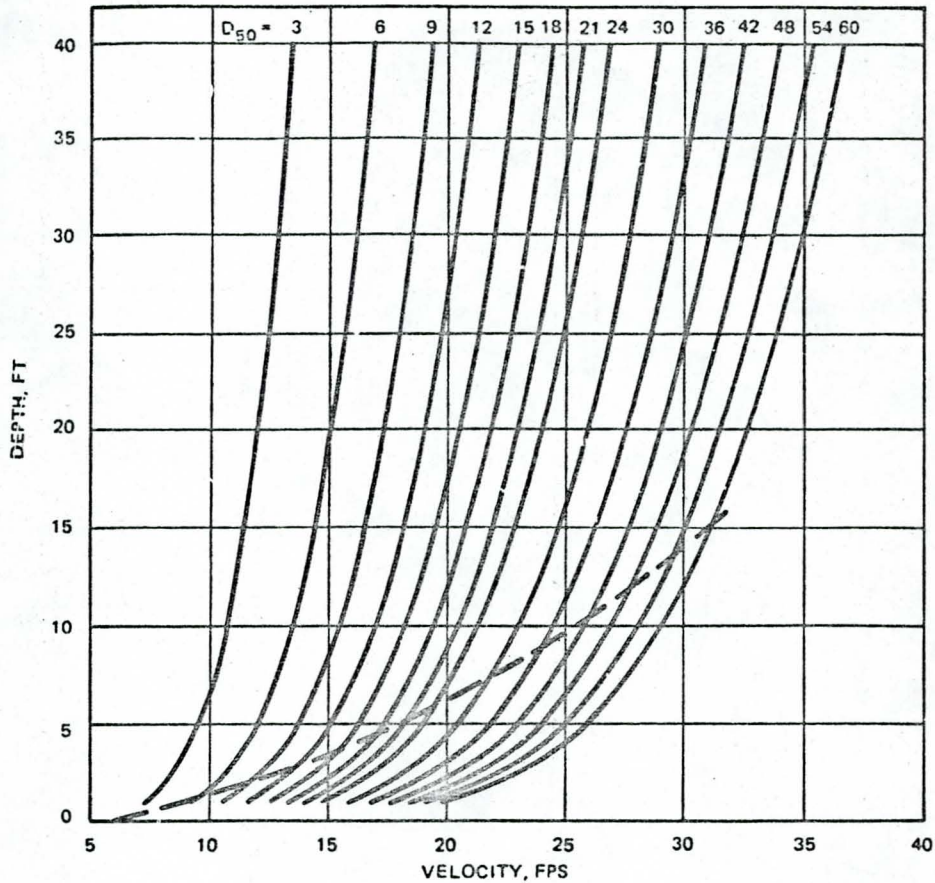
$$\frac{\rho V^2}{(\gamma_s - \gamma) d_{50}} = \left(\frac{1}{1.65 K_F} \right) \left(\frac{D}{d_{50}} \right)^{1/3}$$

NOTE: METHOD LOSES ACCURACY BELOW
DASHED LINE DUE TO FREE SURFACE
EFFECTS

BASE VALUES

$\gamma_s = 165$ LB/CU FT
 $K_F = 0.22$
 LOCAL DEPTH
 MODERATELY ANGULAR STONE
 STRAIGHT CHANNEL
 BED PLACEMENT

**STONE STABILITY
 FROUDE NUMBER CRITERIA
 CRITICAL MEAN VELOCITY
 VS. MEAN DEPTH**



$$\frac{\rho V^2}{(\gamma_s - \gamma) d_{50}} = 63.39 K_t \left(\frac{D}{k_s} \right)^{1/3}$$

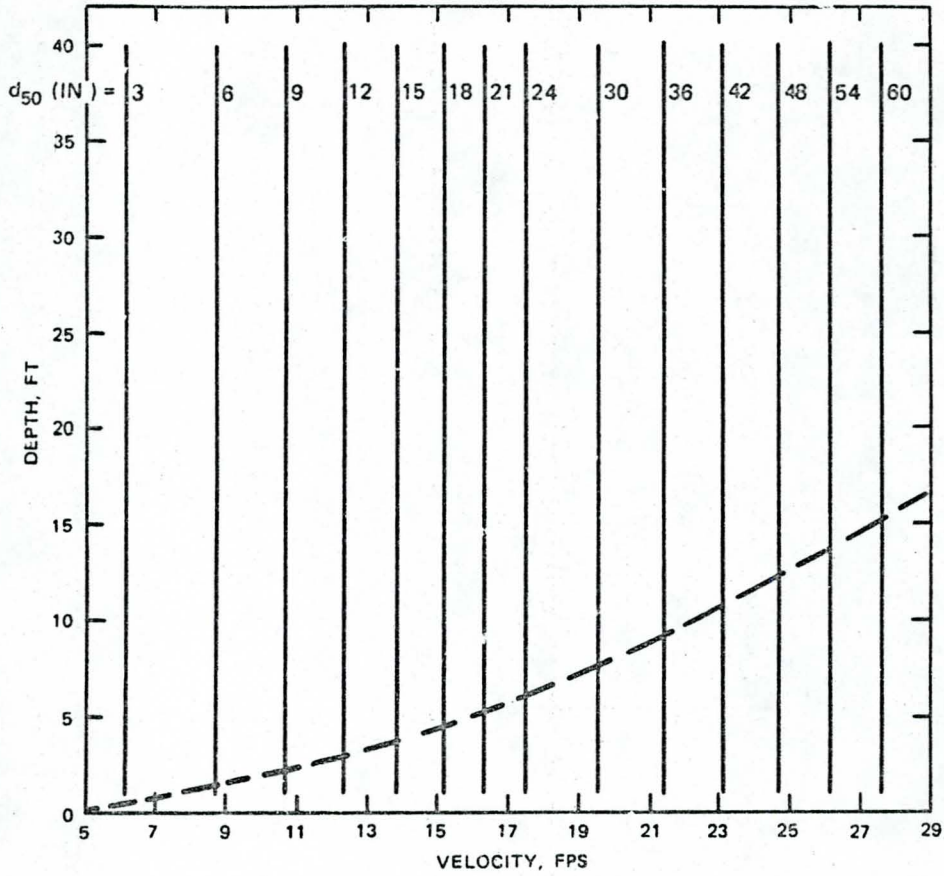
BASE VALUES

$\gamma_s = 165 \text{ LB/CU FT}$
 $K_T = 0.04$
 $k_s = d_{50}$
 LOCAL DEPTH
 MODERATELY ANGULAR STONE
 STRAIGHT CHANNEL
 BED PLACEMENT

NOTE: METHOD LOSES ACCURACY BELOW
 DASHED LINE DUE TO FREE SURFACE
 EFFECTS

STONE STABILITY
TRACTIVE FORCE-POWER PROFILE
CRITICAL MEAN VELOCITY
VS. MEAN DEPTH

PLATE 4



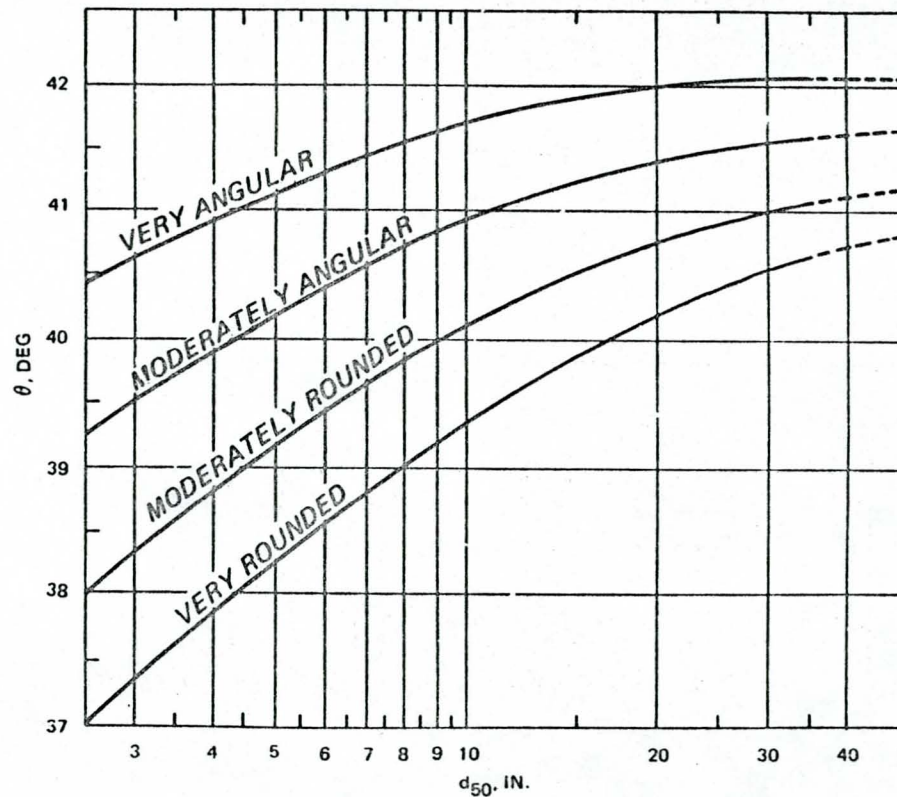
$$\frac{\rho v^2}{(\gamma_s - \gamma)d_{50}} = 2K_1^2$$

NOTE: METHOD LOSES ACCURACY BELOW
DASHED LINE DUE TO FREE SURFACE
EFFECTS

BASE VALUES

$\gamma_s = 165 \text{ LB/CU FT}$
 $K_1 = 1.2$
 MODERATELY ANGULAR STONE
 STRAIGHT CHANNEL
 BED PLACEMENT

STONE STABILITY
 ISBASH CRITERIA
 CRITICAL MEAN VELOCITY
 VS. MEAN DEPTH



RIPRAP DIAMETER
VS.
REPOSE ANGLE
DEVELOPED FROM SIMONS (1957)

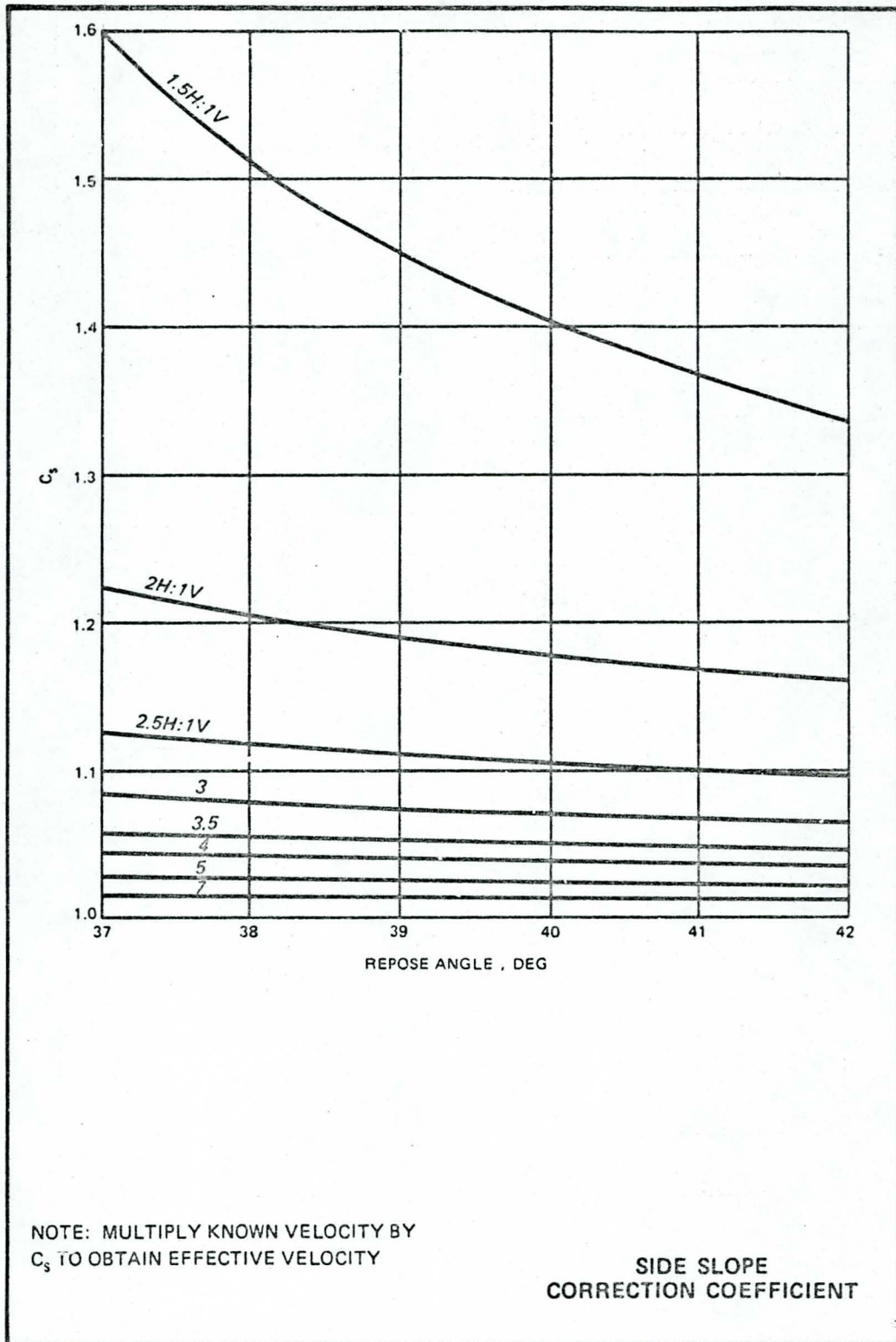
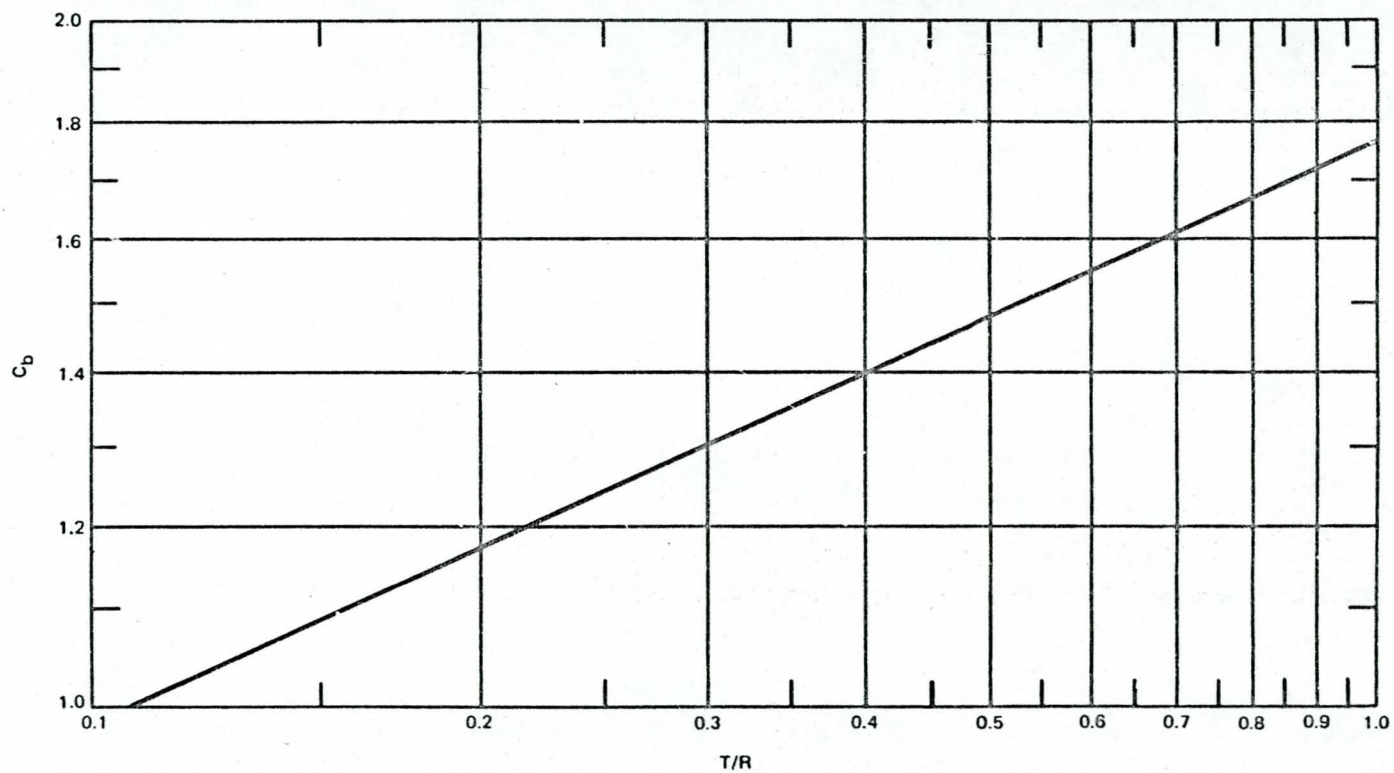
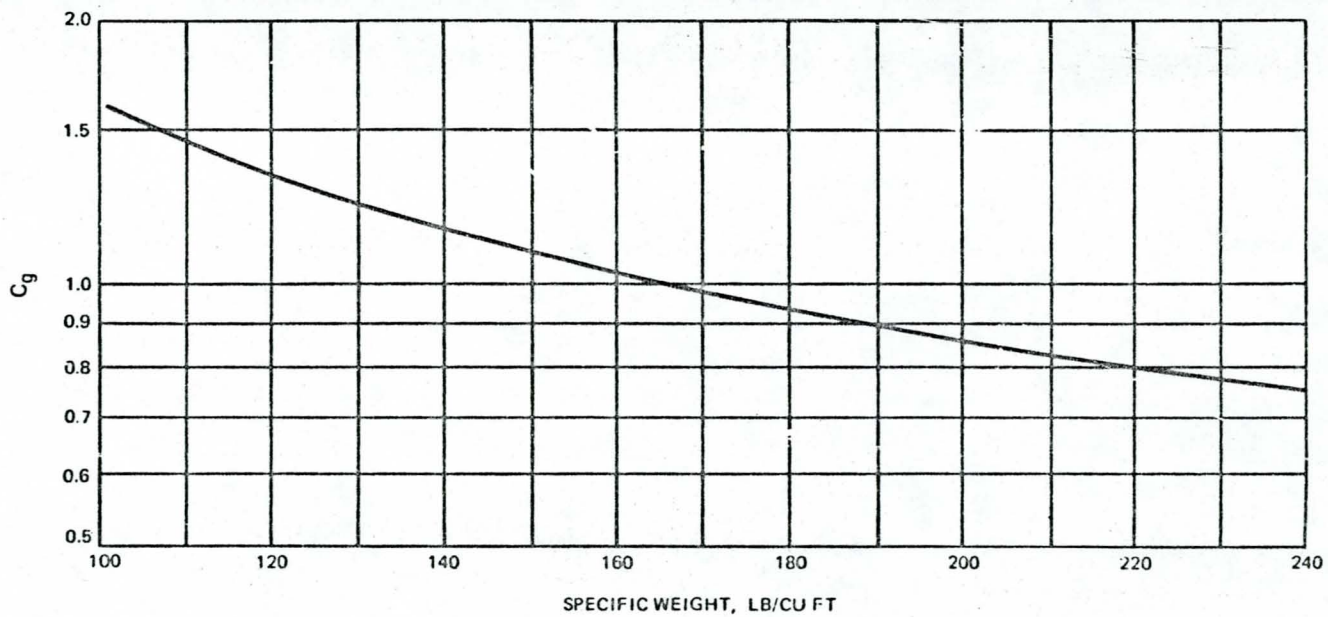


PLATE 8



NOTE: MULTIPLY KNOWN VELOCITY BY C_b
TO OBTAIN EFFECTIVE VELOCITY

BE'ID CORRECTION COEFFICIENT



NOTE: MULTIPLY KNOWN VELOCITY BY C_g
TO OBTAIN EFFECTIVE VELOCITY

SPECIFIC WEIGHT
CORRECTION COEFFICIENT

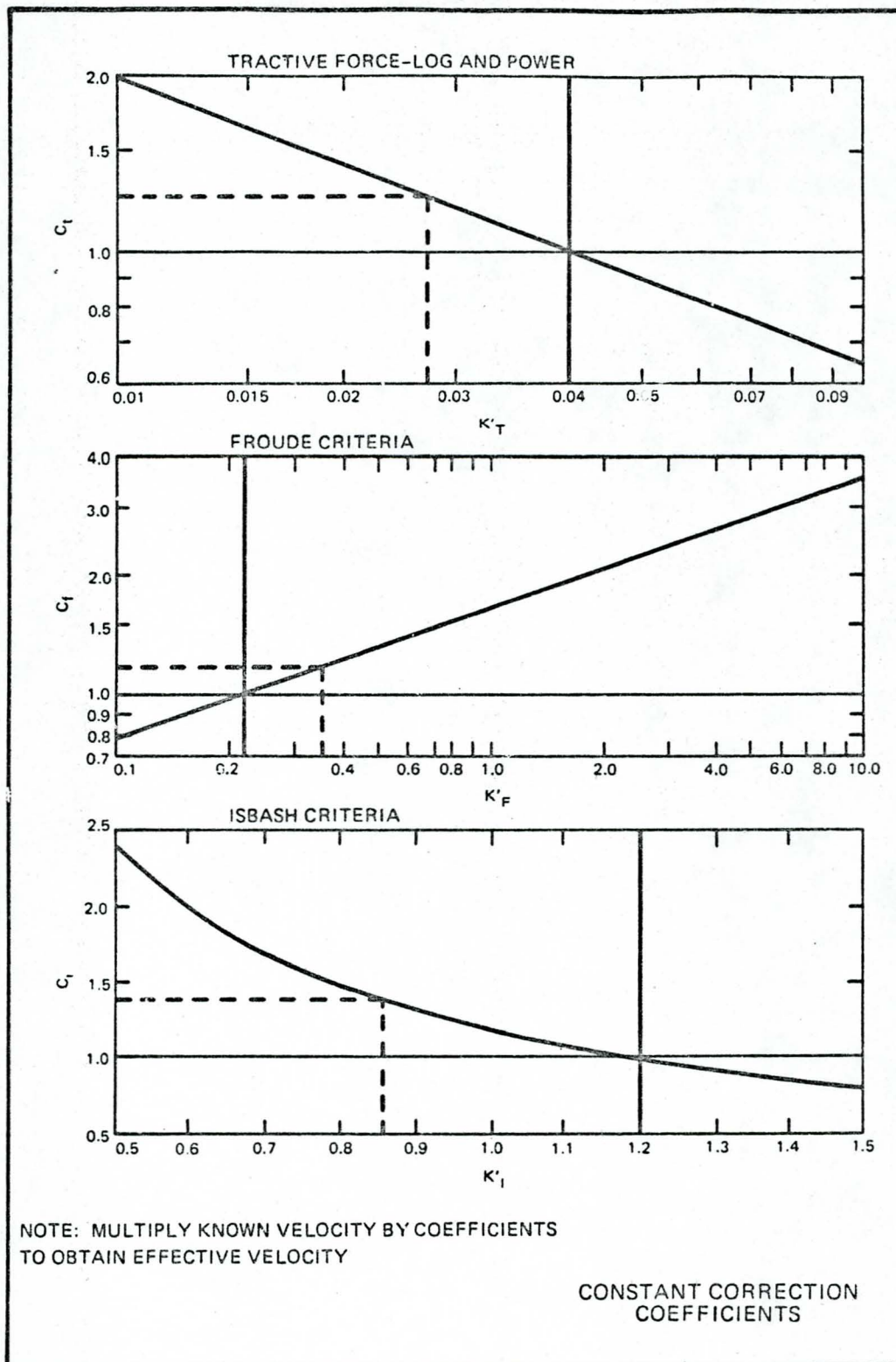
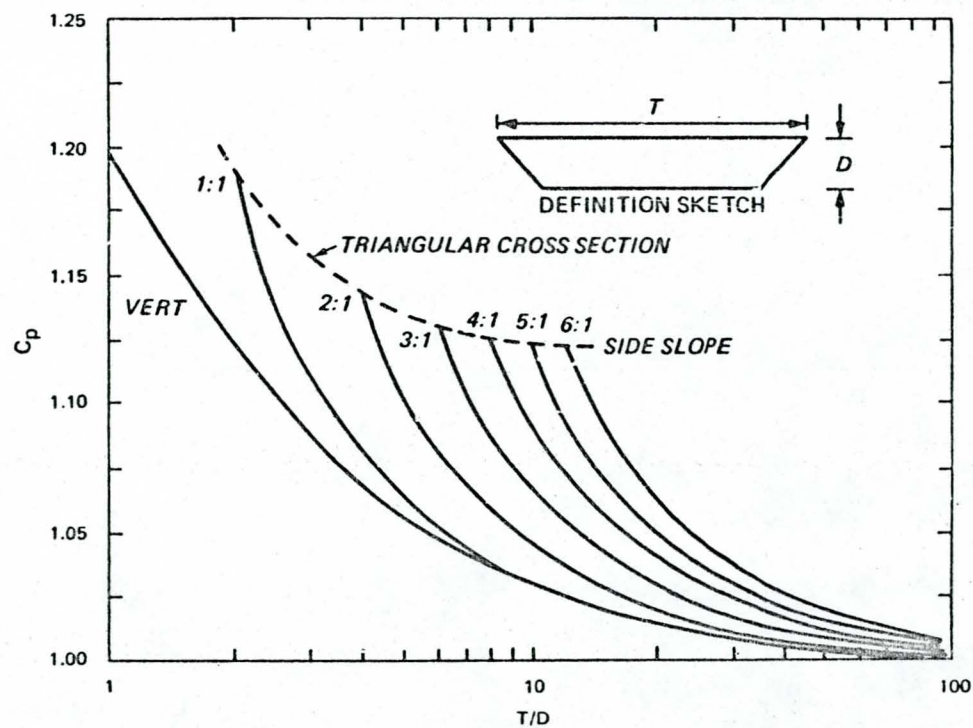


PLATE 10

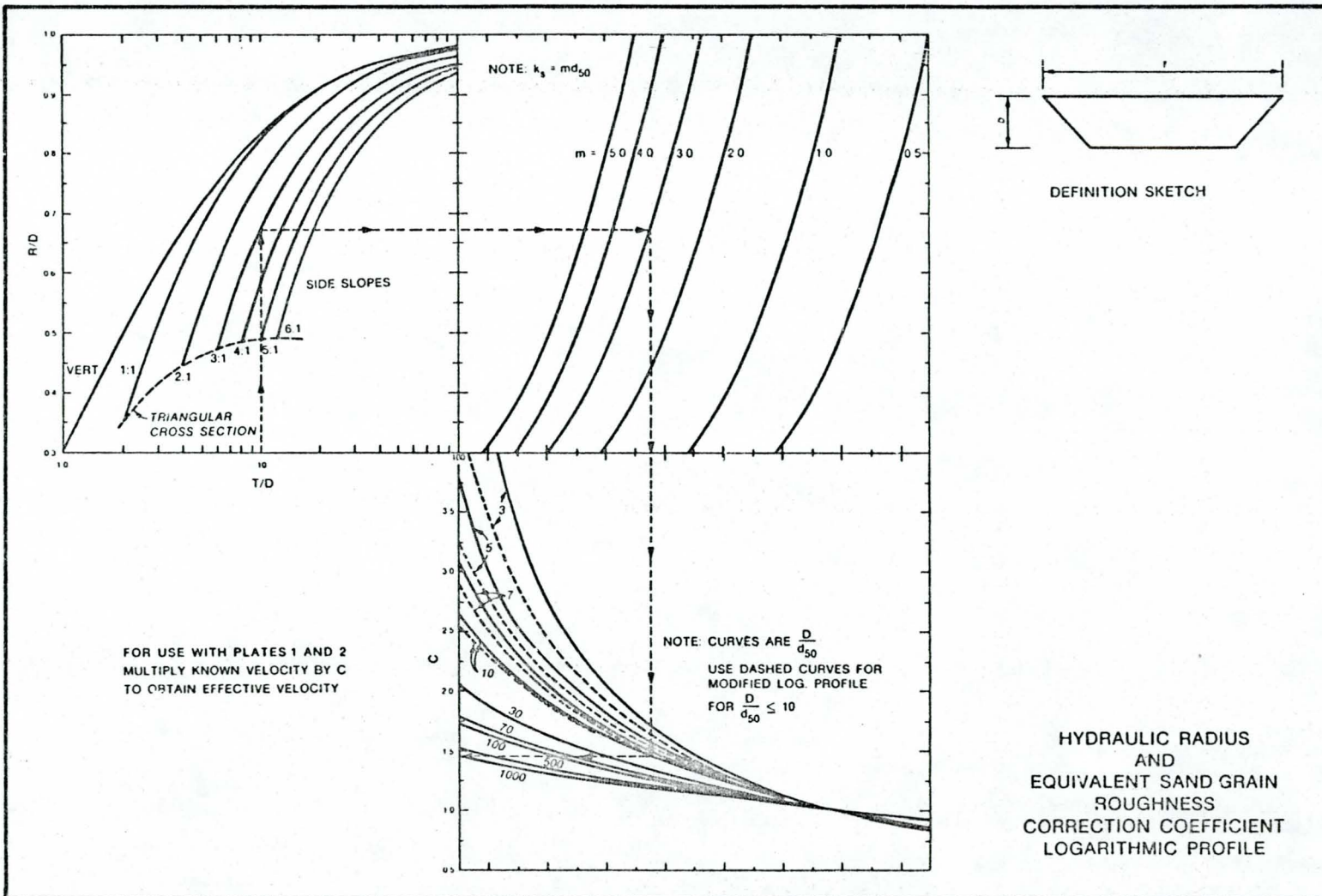


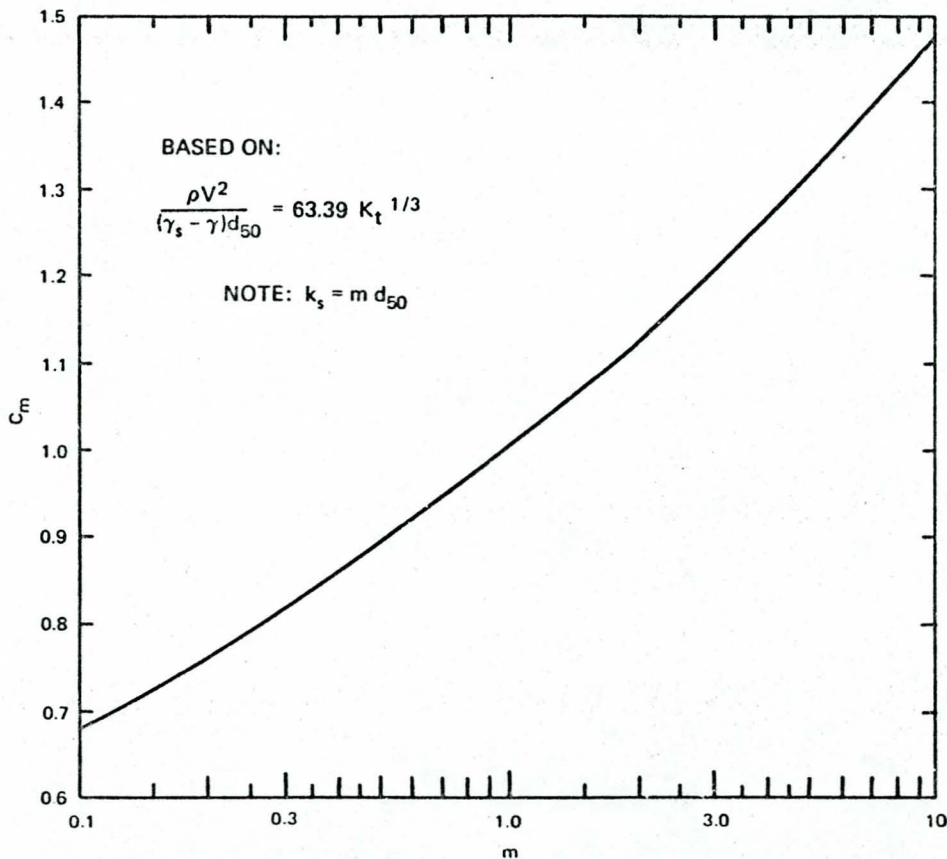
NOTE: FOR USE WITH PLATE 4
 MULTIPLY KNOWN VELOCITY BY C_p TO OBTAIN EFFECTIVE VELOCITY

HYDRAULIC RADIUS
 CORRECTION COEFFICIENT

PLATE 11

PLATE 12





FOR USE WITH PLATE 4

EQUIVALENT SAND GRAIN
 ROUGHNESS
 CORRECTION COEFFICIENT
 POWER PROFILE

MULTIPLY VELOCITY BY C_m TO
 OBTAIN EFFECTIVE VELOCITY

PLATE 13

APPENDIX A: NOTATION

C	Logarithmic profile modification coefficient for hydraulic radius and equivalent roughness
C_b	Coefficient for velocity modification due to a Shields constant using a bend shear
C_f	Correction coefficient for Froude method
C_g	Coefficient for velocity modification due to a Shields constant using a specific weight
C_i	Correction coefficient for Isbash method
C_m	Coefficient for velocity modification due to a Shields constant using a equivalent roughness
C_p	Coefficient for velocity modification due to a Shields constant using a hydraulic radius
C_s	Coefficient for velocity modification due to a Shields constant using a side slope shear
C_t	Coefficient for velocity modification due to a Shields constant using a safety factor
d_{50}	Median stone diameter
D	Depth to top of stone
D'	Depth to a fixed datum, ft
F	Flow Froude number (V/\sqrt{gD})
g	Acceleration of gravity
k_s	Equivalent sand grain roughness of boundary, ft
K_s	Coefficient of side slope shear
K_B	Coefficient for bend shear
K_F	Empirical constant
K'_F	Chosen Froude constant
K_I	Empirical constant
K'_I	Chosen Isbash constant

K_{SF}	Safety factor
K_T	Shield's constant
K'_T	Constant similar to K_T except it includes a safety factor
m	Empirical multiplier
MTFL	Modified tractive force-logarithmic profile
OTFL	Original tractive force-logarithmic profile
p	Multiple of depth such that hydraulic radius $R = pD'$
Q	Discharge
R	Hydraulic radius
R_c	Centerline radius of curvature of bend
SF_F	Shear safety factor for Froude method
SF_T	Shear safety factor for logarithmic and power profile method
T	Top width of channel entering bend
TFP	Tractive force-power profile
U_b	Velocity on the stone
v	Local mean velocity in the vertical
V	Mean channel velocity
V_{eff}	Effective velocity
γ	Specific weight of water
γ_s	Specific weight of stone
γ'_s	Specific weight of stone other than base condition
θ	Riprap angle of repose
ρ	Mass density of water
τ_b	Shear in a bend, lb/ft^2
τ_c	Critical tractive force
$\tau_{c_{eff}}$	Critical shear adjusted for specific weight and side slope placement

- $\bar{\tau}_0$ Average boundary shear, lb/ft²
- $\bar{\tau}_{0\text{eff}}$ Actual shear adjusted for channel shape, bend, equivalent roughness, and safety factor
- τ_s Side slope critical shear, lb/ft²
- τ_{SF} Actual shear with a safety factor applied
- ϕ Side slope angle

END

DATE

FILMED

8-88

DTIC